A THEORY FOR CIRCULAR PLATES USING HIGHER ORDER APPROXIMATIONS

K.T. SUNDARA RAJA IYENGAR, K. CHANDRASHEKHARA, V.K. SEBASTIAN*

Civil Engineering Department,
Indian Institute of Science, Bangalore-12, India

(On leave from Department of Civil Engineering, College of Engineering, Trivandrum, India)*

SUMMARY

A higher order theory for thick axi-symmetric circular plates which is an extension of Reissner's shear deformation theory is presented using a variational approach. This consists in assuming a stress and displacement field which satisfies the physical requirements of the problem as nearly as possible. Thus starting with an assumed displacement field in the form of a higher order truncated polynomial in the thickness co-ordinate, (the coefficients being arbitrary functions of the other variables), and a consistent stress state satisfying the boundary conditions on the top and bottom faces of the plate, the governing equations and the associated boundary conditions along the edges are obtained through the variational theorem of Reissner. The resulting equations are such that the symmetric and anti-symmetric parts can be treated separately. Such a procedure of taking higher order truncated polynomials for displacement and stress states does not seem to have appeared in the literature on thick plates.

By suitably combining and manipulating these equations, governing equations in higher order shear stress coefficients are obtained for both symmetric and anti-symmetric problems. Once these equations are solved the solution is complete as all other unknowns can be written in terms of these shear stress coefficients. The method is applied to uniformly loaded solid and annular circular plates.

To get an idea of the accuracy of the method numerical results obtained by this method are compared with those from an elasticity solution for plates under self-equilibrating normal loads. Comparisons have shown that the present method gives reasonably good agreement with elasticity solution even for a thick plate with diameter-to-thickness ratio 2. Detailed numerical results are obtained and compared with classical and Reissner theories for uniformly loaded circular plates for various diameter to thickness ratios and for three different Poisson's ratios (viz. $\nu = 0.3$, 0.2 and 0.1). Both simply supported and clamped edge conditions are considered. Numerical results are also included for annular plates for various ratios of outer to inner diameter of the plate for a given thickness to outer diameter ratio.

1. Introduction

The classical theory of plates is sufficiently accurate for many engineering problems. However there are many cases where the classical theory is found inadequate to represent stresses and deformations. This is true especially if the plate is thick or if it is subjected to concentrated forces in which case the results of the classical theory in the immediate vicinity of the loads will be very much in error.

In recent years a number of plate theories have been developed in an effort to extend the range of validity of the classical theory to that of thicker plates by including the effects of transverse shear and normal stress, etc. One of the foremost theory to include shear deformation has been due to Reissner [1]. In this theory a system of differential equations which take into account the transverse shear deformability of of the plate has been derived through a variational approach. Hencky, Bolle, Schäfer, Kromm, Mindlin and Volterra [2, 3, 4, 5, 6, 7], have presented new theories that take into account the effect of shear. In these theories one generally starts from hypothesis concerning stress (or displacement) distribution in the plate in order to reach equations of equilibrium.

Starting from the three-dimensional elasticity equations Love [8] has developed a theory for thick plates. Neglecting the edge boundary conditions he has developed a solution which is valid only in the region away from the edges. Donnell and Lee [9, 10] have given a theory suitable for thick plates. The solution, in the form of infinite series involving derivatives of loading, satisfies the three dimensional elasticity equations more and more exactly as the number of terms in the series type solution increases. Lee and Lee and Conlee [11, 12] have respectively applied the theory to rectangular and circular plates.

Reissner's shear deformation theory (of the sixth order in the general case) is of the fourth order for axi-symmetric problems. The governing differential equation in the mid-surface deflection differs from the corresponding classical theory equation only by an additional term containing the derivative of loading in the right hand side. Though the expressions for moments and shear are accordingly different the earlier investigations [13] have shown that the overall improvement obtained is not considerable. Hence a higher order theory for axi-symmetric circular plates is presented here. Starting with appropriate and rational stress and displacement fields, use is made of Reissner's variational equation [14] to arrive at the governing equations and the associated boundary conditions. The equations are such that the symmetric and anti-symmetric parts (with respect to the middle plane) can be treated separately. The equations are reduced to fourth order ordinary differential equations in higher order shear stress coefficients,

the solutions of which are written in terms of Bessel functions of complex arguments. In order to get an idea of the accuracy achieved numerical results obtained from the higher order theory are compared with those of the elasticity solution of Chandrashekhara [15] for a plate subjected to self-equilibrating normal loads. Results for uniformly loaded clamped and simply supported plates have been presented for various thickness to diameter ratios and for different Poisson's ratios. Results have also been included for an uniformly loaded annular plate whose inner edge is free and outer edge is clamped. Numerical results have been compared with those of classical and Reissner theories.

2. Analysis

The approach indicated by Reissner [14] consists in assuming suitable stress and displacement fields which satisfy the physical requirements of the problem as nearly as possible. The governing equations and associated boundary conditions are then obtained by the application of the variational equation.

The variational equation of Reissner [14] is:

$$\delta \left\{ \iiint_V F \, dV - \iint_{S_1} (\bar{p}_r \, u + \bar{p}_\theta \, v + \bar{p}_z \, w) \, dS \right\} = 0 \qquad (1)$$

where

F = $\sigma_r \varepsilon_r + \sigma_\theta \varepsilon_\theta + \ldots\ldots + \sigma_{\theta z} \varepsilon_{\theta z} - W$

W = Strain energy density function defined as $\varepsilon_r = W/\sigma_r$ etc.

σ_s = stress components

u, v, w = displacement components

$\bar{p}_r, \bar{p}_\theta, \bar{p}_z$ = applied surface tractions in the r, θ, z directions respectively.

A displacement state is taken in the form of higher order polynomials in z as:

$$u = u_0 + u_1 z + u_2 z^2 + u_3 z^3$$
$$w = w_0 + w_1 z + w_2 z^2 \qquad (2)$$

where coefficients u_0, u_1, etc. are functions of r only.

A stress state consistent with the assumption of eq.(2) must now be obtained. This can be achieved by modifying the classical forms by assuming higher order polynomials in z, the coefficients of these polynomials being arbitrary functions of r. These polynomials should be such that the resulting stress-state comply with the definition of classical stress resultants and should satisfy the boundary conditions on the top and bottom faces of the plate. For a plate subjected to normal loads

(Fig. 1) the transverse shearing stress must vanish on these faces and the transverse normal stress must be equal to the applied normal loads. Thus the stress state becomes:

$$\sigma_r = N_r/h + 12\, M_r\, z/h^3 + R_r\, f_1(z)/h^3 + P_r\, z\, f_2(z)/h^5$$

$$\sigma_\theta = N_\theta/h + 12\, M_\theta\, z/h^3 + R_\theta\, f_1(z)/h^3 + P_\theta\, z\, f_2(z)/h^5 \qquad (3)$$

$$\sigma_{rz} = 3\, V_r(1-4z^2/h^2)/2h + A_r\, z\, f_3(z)/h^3 + B_r\, f_4(z)/h^5$$

$$\sigma_z = q\,(-1+3\, z/h - 4\, z^2/h^3)/2 + 3\, S\, f_5(z)/28\, h + T\, z\, f_5(z)/h^3$$

where

$$f_1(z) = 15\,(1-12\, z^2/h^2)\,, \quad f_2(z) = -420\,(1-20\, z^2/3h^2)$$

$$f_3(z) = 15\,(1-4z^2/h^2)\,, \quad f_4(z) = 35\,(1-24\, z^2/h^2 + 80\, z^4/h^4)/4$$

$$f_5(z) = 35\,(1-8\, z^2/h^2 + 16\, z^4/h^4)/4$$

$N_r, M_r, \ldots\ldots, T$ are functions of r only.

Since eq.(2) consists of finite polynominals in z they are not the most general representation of displacements. If the last two terms in each of the eqs. (2) and (3) are deleted, the resulting displacement and stress fields correspond to Reissner's theory. This may be designated as a first order theory. Then the present theory as per eqs. (2) and (3) which incorporates two higher order effects (one even and one odd) over Reissner's may well be termed as a third order theory.

2.1 Governing Equations and Boundary Conditions:

2.1.1 Governing differential equation:

The displacements and stresses are now substituted into eq. (1). Performing integrations with respect to z and carrying out the variations yield the governing equations and associated boundary conditions. The governing equations are 14 first order ordinary differential equations plus four algebraic equations which by suitably combining and manipulating are reduced to the following higher order equations convenient for integration.

$$LL(A_r) - \frac{24}{h^2}\, L(A_r) + \frac{504}{h^4}\, A_r = \frac{7}{10h}\, \frac{dq}{dr}$$

$$L(\bar{u}) + \frac{\mu(1+\mu)}{2\, Eh}\, L(A_r) = \frac{\mu(1+\mu)}{2\, Eh}\, \frac{dq}{dr} \qquad (4)$$

$$LL(B_r) - \frac{1008}{11\, h^2}\, L(B_r) + \frac{45360}{11\, h^4}\, B_r = \frac{64.8}{11}\, \frac{dq}{dr} - \frac{3.6}{11}\, h^2\, L\left(\frac{dq}{dr}\right)$$

$$dV_r/dr + V_r/r = -q$$

$$D\,L(\bar{u}^*) + \frac{\mu}{10(1-\mu)}\,h^2\,\frac{dq}{dr} + \frac{\mu}{6(1-\mu)}\,L(B_r) = V_r$$

$$\frac{dw^*}{dr} + \bar{u}^* - \frac{12}{5}\,\frac{(1+\mu)}{E\,h}\,V_r + 4\,\frac{(1+\mu)}{Eh^3}\,B_r = 0 \qquad (5)$$

where

$$L = \left(\frac{d^2}{dr^2} + \frac{1}{r}\,\frac{d}{dr} - \frac{1}{r^2}\right),\quad D = Eh^3/12\,(1-\mu^2)$$

$$\bar{u} = u_o + u_2\,h^2/6,\quad \bar{u}^* = u_1 + 3\,h^2\,u_3/20,\quad w^* = w_o + h^2\,w_2/12$$

2.1.2 Boundary Conditions:

The variational equation also gives the natural boundary conditions. These are, (say for an edge r = constant) either the quantities

$$N_r,\ M_r,\ R_r,\ P_r,\ V_r,\ A_r \text{ and } B_r$$

or the corresponding displacement coefficients

$$u_o,\ u_1,\ u_2,\ u_3,\ w_o,\ w_1 \text{ and } w_2$$

be prescribed.

From eqs. (2) and (3) it can be seen that boundary conditions correspond to the following stress (or displacement) conditions:

$$\sigma_r = 0 \text{ (or } u = 0),\quad \sigma_{rz} = 0 \text{ (or } w = 0)$$

The boundary conditions for different supports are

(a) for clamped edges: $\bar{u} = u_1 = \bar{u}^* = u_3 = w^* = w_1 = w_2 = 0$ (6)

(b) for simply supported edges:

$$N_r = M_r = R_r = P_r = w^* = w_1 = w_2 = 0 \qquad (7)$$

and (c) for free edges: $N_r = M_r = R_r = P_r = V_r = A_r = B_r = 0$ (8)

2.2 Solution:

The homogeneous part of the fourth order eqs. (4) and (5) are of the same form and can be written as:

$$LL(F) - \delta^2\,L(F) + \beta^4(F) = 0 \qquad (9)$$

The general solution of (9) can be written as

$$F = A_1\,J_o\,(\sqrt{\eta_1}\,r) + A_2\,H_o^{(1)}\,(\sqrt{\eta_1}\,r)$$

$$+ A_3\,J_o\,(\sqrt{\eta_1}\,r) + A_2\,H_o^{(2)}\,(\sqrt{\eta_1}\,r) \qquad (10)$$

where η_1 and $\bar{\eta}_1$ are the roots of the equation

$$\eta^2 + 2\,\delta^2\eta + \beta^4 = 0$$

J_o = Bessel functions of the first kind and zero order

$H_o^{(1)}$, $H_o^{(2)}$ = Hankel functions of the first and second kind of zero order respectively.

It is convenient to write:

$$\sqrt{\eta_1} = \beta\, e^{i\varphi} = \beta\,(\cos\varphi + i \sin\varphi)$$

$$\sqrt{\bar{\eta}_1} = \beta\, e^{-i\varphi} = \beta\,(\cos\varphi - i \sin\varphi)$$

Since the functions $J_o(\sqrt{\eta_1}\, r)$ etc. are complex while the plate-deflection and resultants must be real. $A_1, .., _4$ must be complex. In order to express the solution through real functions eq.(10) is written in the following form:

$$F = C_1\, u_o(\beta r) + C_2\, v_o(\beta r) + C_3\, f_o(\beta r) + C_4\, g_o(\beta r) \qquad (11)$$

where

$$u_o(\beta r) = \text{Re}\, J_o(\sqrt{\eta_1}\, r), \quad v_o(\beta r) = \text{Im}\, J_o(\sqrt{\eta_1}\, r)$$

$$f_o(\beta r) = \text{Re}\, H_o^{(1)}(\sqrt{\eta_1}\, r), \quad g_o(\beta r) = \text{Im}\, H_o^{(2)}(\sqrt{\bar{\eta}_1}\, r)$$

The constants $C_1, .., _4$ are now real.

The remaining equations of (4) and (5) are readily integrable.

3. Applications:

The method is applied to the following problems.

3.1 Uniformly loaded annular plate with clamped outer edge and free inner edge (Fig. 1).

All the derivatives of q in the governing equations vanish. The integration of eqs. (4) and (5) and further substitution of results in appropriate equations yield the following final expressions for the unknowns of the problem. The symmetric and anti-symmetric parts are independent and hence are given separately. The following notations are introduced:

$$\Theta_1 = \beta(u_o \cos\varphi - v_o \sin\varphi), \quad \Theta_2 = \beta(u_o \sin\varphi + v_o \cos\varphi)$$

$$m_1 = \beta^2(u_1 \cos 2\varphi - v_1 \sin 2\varphi), \quad m_2 = \beta^2(u_1 \sin 2\varphi + v_1 \cos 2\varphi)$$

$$n_1 = \beta^3(u_o \cos 3\varphi - v_o \sin 3\varphi), \quad n_2 = \beta^3(u_o \sin 3\varphi + v_o \cos 3\varphi)$$

$f_1, .., _4 = u_1, v_1, f_1$ and g_1 respectively.

The functions Θ_3, Θ_4, m_3, m_4, etc. can be obtained from above by replacing u, v by f and g respectively.

3.1.1 Symmetric-part:

$$A_r = \sum_{i=1}^{4} C_i f_i, \quad \bar{u} = A_o r - \frac{\mu(1+\mu)}{2\,Eh} A_r + \frac{B_o}{r^2}$$

$$w_1 = -2\frac{\mu}{1-\mu} A_o + \sum_{i=1}^{4} C_i m_i - \frac{1-\mu-2\mu^2}{2(1-\mu)} q, u_2 = \sum_{i=1}^{4} C_i H_i(\beta r)$$

$$N_r = \frac{A_o}{1-\mu} + \frac{\mu}{2}\frac{A_r}{r} - \frac{B_o}{1+\mu}\frac{1}{r^2} - \frac{\mu}{2(1-\mu)} q \qquad (12)$$

$$N_\theta = \frac{A_o}{1-\mu} + \frac{B_o}{1+\mu}\frac{1}{r^2} + \frac{\mu}{2}\sum_{i=1}^{4} C_i \Theta_i - \frac{\mu}{2(1-\mu)} q$$

$$R_r = \sum_{i=1}^{4} C_i R_i(\beta r), \quad R_\theta = \sum_{i=1}^{4} C_i R_{\theta i}(\beta r)$$

where

$$H_i(\beta r) = a_1 \frac{m_i}{Eh} + \frac{30}{7}\frac{(2+\mu-\mu^2)}{Eh^3} f_i$$

$$M_i(\beta r) = \frac{\mu\, a_1}{21(\mu-1)}\frac{h}{E} n_i + \left(\frac{70+40\mu-29\mu^2}{98}\right)\frac{\Theta_i}{Eh}$$

$$R_i(\beta r) = \frac{h^4 a_1}{180(1-\mu^2)}\left[n_i - (1-\mu)\frac{m_i}{r}\right] + \frac{h^2}{21}\Theta_i - \frac{2-\mu}{42} h^2 \frac{f_i}{r}$$

$$R_{\theta i}(\beta r) = \frac{h^4 a_1}{180(1-\mu^2)}\left[\mu n_i + (1-\mu)\frac{m_i}{r}\right] + \frac{\mu h^2}{42}\Theta_i + \frac{2-\mu}{42} h^2 \frac{f_i}{r}$$

$$a_1 = \frac{5}{14} - \frac{69}{196}\mu^2, \quad \beta = 4.7381, \quad \varphi = 1.0699$$

3.1.2 Anti-symmetric part:

The constants and functions appearing in this are different from those of the symmetric part. The primes over them are omitted for convenience.

$$B_r = \sum_{i=1}^{4} C_i f_i, \quad V_r = -\frac{q}{2r}(r^2-b^2)$$

$$u^* = A_o r + \frac{B_o}{r} - \frac{2\mu(1+\mu)}{Eh^3} B_r - \frac{qr^3}{16D} + \frac{qb^2}{8D} r(2\log r/a - 1)$$

$$u_3 = \sum_{i=1}^{4} C_i H_i(\beta r) + \frac{(2+\mu-\mu^2)}{Eh^3} q\,(r - b^2/r)$$

$$w_2 = -\frac{\mu}{1-\mu} A_o + \sum_{i=1}^{4} C_i M_i(\beta r) + \frac{\mu}{8(1-\mu)}\frac{qr^2}{D}$$

$$+\left(\frac{2}{3} - \frac{4}{3}\frac{\mu^2}{1-\mu} + \frac{\mu(1+\mu)(2-\mu)}{15(1-\mu)}\frac{q}{Eh} - \frac{\mu}{1-\mu}\frac{qb^2}{4D}\log(r/a)\right.$$

$$M_r = D(1+\mu)\, A_o - D(1-\mu)\, \frac{B_o}{r^2} + \frac{\mu}{6}\, \frac{B_r}{r} + \frac{\mu}{10(1-\mu)}\, q$$

$$-(3+\mu)\, \frac{qr^2}{16} + \frac{qb^2}{4}\,(1+\mu)\, \log r/a + (1-\mu)\, \frac{qb^2}{8} \qquad (13)$$

$$M_\theta = D(1+\mu)\, A_o + D(1-\mu)\, \frac{B_o}{r^2} + \frac{\mu}{6} \sum_{i=1}^{4} C_i\, (\theta_i - \frac{f_i}{r})$$

$$+ \frac{\mu}{10(1-\mu)}\, q - (1+3\mu)\, \frac{qr^2}{16} + (1+\mu)\, \frac{qb^2}{4} \log r/a - (1-\mu)\, \frac{qb^2}{8}$$

$$P_r = \sum_{i=1}^{4} C_i\, P_i\, (\beta r) + \frac{2+\mu}{2800}\, qh^4 + \frac{2-\mu}{2800}\, qh^4\, \frac{b^2}{r^2}$$

$$P_\theta = \sum_{i=1}^{4} C_i\, P_{\theta i}\, (\beta r) + \frac{2+\mu}{2800}\, qh^4 - \frac{2-\mu}{2800}\, qh^4\, \frac{b^2}{r^2}$$

where

$$H_i\,(\beta r) = a_1\, \frac{m_i}{Eh^3} + \frac{280}{9}\, \frac{2+\mu-\mu^2}{Eh^5}\, f_i$$

$$M_i\,(\beta r) = \left[\frac{70}{33} + \frac{(56-55\mu-\mu^2)\mu}{27(1-\mu)}\right] \frac{\theta_i}{Eh^3} + \frac{1}{30}\, \frac{\mu}{1-\mu}\, a_1\, \frac{n_i}{Eh}$$

$$P_i\,(\beta r) = \frac{h^4}{2800(1-\mu^2)}\, a_1\, [n_i - (1-\mu)\, \frac{m_i}{r}] + \frac{h^2}{45}\, \theta_i - \frac{2-\mu}{90}\, h^2\, \frac{f_i}{r}$$

$$P_{\theta i}(\beta r) = \frac{h^4}{2800(1-\mu^2)}\, a_1\, [\mu\, n_i + (1-\mu)\, \frac{m_i}{r}] + \frac{\mu h^2}{90}\, \theta_i + \frac{2-\mu}{90}\, h^2\, \frac{f_i}{r}$$

$$a_1 = (\frac{70}{99} - \frac{55}{81}\, \mu^2),\ \beta = 8.01,\ \varphi = 1.18246.$$

The integration constants in eqs. (12) and (13) are determined using appropriate boundary conditions given in eqs. (6) and (8).

Numerical results for annular plates having inner to outer radii ratio (b/a) varying from 0.1 to 0.5 and outer radius to thickness ratio (a/h) varying from 2 to 15 have been obtained. Fig. 2 shows variation of maximum non-dimensional deflection while Fig. 3 shows variation of maximum tangential stress (at point A).

3.2 Uniformly loaded solid plates:

Expressions for a solid plate can be obtained from those of the annular plate by deleting the terms containing B_o and b in eqs. (12) and (13) and also by restricting i to land 2.

Numerical results for clamped and simply supported plates were obtained for a/h ratios varying from 1 to 5 and Poisson's ratio μ = 0.1, 0.2, and 0.3. Fig. 4(a) shows the distribution of radial stress (σ_r/q) at the centre of the plate while Fig. 4(b) shows the same at the edge for

a/h = 1. Fig. (5) shows shear stress distribution (σ_r/q) at different sections for a/h = 1, 2 and 5. Figs. (6) and (7) show the variation of maximum deflection and radial stress for different a/h & Poisson's ratios.

In Figs. 2 to 5 results obtained from classical and 1st order (Reissner) theories have also been incorporated for comparison.

3.3 Plate with self-equilibrating load (Fig. 8):

The solution for the region $0 \leq r \leq c$ (solid plate) and that for the region $c \leq r \leq a$ (annular plate) can be obtained from eqs. (12) and (13). The constants are obtained using boundary conditions at r = a and continuity conditions at r = c. At the junction (r = c) there are fourteen equations expressing the continuity of u_0, u_1, u_2, u_3, w_0, w_1, w_2, N_r, M_r, R_r, P_r, V_r, A_r and B_r.

Numerical results for different a/h ratios have been obtained for c/a ratio of 0.125. The radial stress profile at the centre is given in Fig. 9 while the variations of radial and tangential stress at the top surface are given in Figs. 10 and 11 respectively. Results from an elasticity solution [15] and classical theory are included for comparison.

4. Discussion of numerical results:

It may be observed from Figs. 2 and 3 that for a/h = 2 and for all b/a ratios there is considerable difference between the first order (Reissner's) theory and third order theory results both for deflection and tangential stress. This indicates that if the radius of the hole is very much less than the thickness of the plate, then for such a case the results obtained using first order theory could be in error.

It may be seen from Figs. 4(a) and (b) that the radial stress distribution is far from linear and this may be due to combined thickness and edge effect. It was observed that for larger a/h ratios (thinner plates) the variation of radial stress at the centre approaches the linear distribution of classical theory.

From Fig. 5 it may be observed that for sections close to the support the shear stress distribution deviates considerably from the classical parabolic distribution. It was also observed that for larger a/h ratios (a/h = 5), the classical parabolic distribution of shear stress can be achieved even at sections very close to the support (r/a = 0.90).

From Figs. 6 and 7 it may be observed that Poisson's ratio has a considerable effect on deflection and stresses. However, Poisson's ratio was found to have negligible effect on normal stress (σ_z). It must be mentioned here that similar deviations were also observed for simply supported case.

Figs. 9, 10 and 11 show that classical and third order theory give almost the same radial stress distribution as given by elasticity solution for a/h = 5. However for a/h less than 5 the deviations between the classical and third order theories are considerable. It is interesting to note that the results of 3rd order theory for the radial stress distribution even for a/h = 1 agrees fairly well with those of elasticity solution (Fig. 4a). The deviations are more predominant at the centre of the plate than at the edges as seen in Figs. 10 and 11. The percentage deviations between classical, Reissner, 3rd order and elasticity theories (for maximum radial stress at centre) are shown in Fig. 12. The percentage deviation is calculated from

$$\% \text{ deviation} = \frac{\text{Elasticity solution - 3rd order(or 1st order or classical) solution}}{\text{Elasticity solution}}$$

From this figure it may be observed that for a/h = 1 the percentage difference between elasticity and 3rd order theory is 16, while those between elasticity and 1st order and classical theories are respectively 50 and 90, thus indicating that the third order theory could give results close to elasticity solution.

References

[1] REISSNER, E., "The effect of transverse shear deformation on the bonding of elastic plates", Jl. Appl. Mech., 12, A69 (1945).

[2] HENCKY, H., "Über die Berucksichtigung der Schubverzerung in ebenen Platten", Ing. Archiv, 56, 72 (1947).

[3] BOLLE, L., "Contribution au probleme lineaire deflexion dune plaque elastique", Bulletin Technique de la Suisse Romande, 27, 281 (1947).

[4] SCHÄFER, M., "Über eine Verfeinerung der Klassichen Theorie dünner schwahgebegener Platten", ZAMM, 16, 161 (1952).

[5] KROMM, A., "Über die Randquerkräfte bei gestützten Platten", ZAMM, 35, 231 (1955).

[6] MINDLIN, R.D., "Influence of rotatary inertia and shear on flexural motions of isotropic elastic plates", Jl. Appl. Mech., 31, (1951).

[7] VOLTERRA, E., "Method of internal constraints and its application", Trans. ASCE, 128, 509 (1963).

[8] LOVE, A.E.H., Mathematical Theory of Elasticity , Dover Publications, (1952).

[9] DONNEL, L.H., "A theory for thick plates", Proc. Second U.S.National Cong. Appl. Mech., 369 (1954).

[10] DONNEL, L.H., LEE, C.W., "A study on thick plates under tangential loads applied on the faces", Proc. Third U.S. National Cong. Appl. Mech., 401 (1958).

[11] LEE, C.W., "Three dimensional solution for simply supported thick rectangular plates", Mech. Engg. Design, 6, 155 (1967).

[12] LEE, C.W., CONLEE, G.D., "Bending and twisting of thick plates with a circular hole", Jl. Franklin Inst., 285, 377 (1968).

[13] LEHNHOFF, T.F., MILLER, R.E., "Influence of transverse shear on the small displacement theory of circular plates", AIAA Jl., 7, 1499 (1965).

[14] REISSNER, E., "On a variational theorem in elasticity", Jl.Maths. and Phys., 29, 90 (1950).

[15] CHANDRASHEKHARA, K., "A note on finite solid cylinders", AIAA Jl., 7, 1161 (1969).

[16] KLOSNER, J.M., LEVINE, H.S., "Further comparisons of elasticity and shell theory solutions", AIAA Jl., 4, (1966).

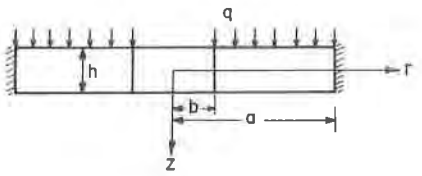

Fig. 1 Co-ordinate axes and loading

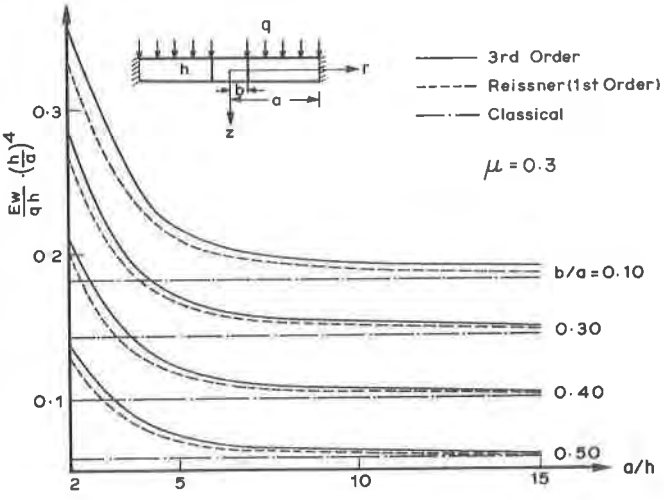

Fig. 2 Variation of maximum non-dimensional deflection

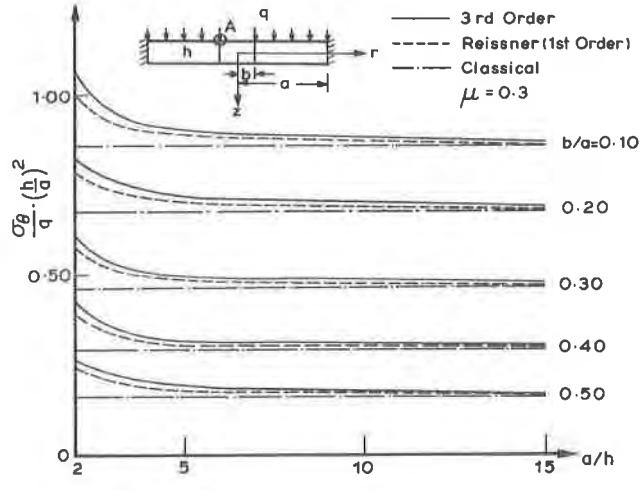

Fig. 3 Variation of non-dimensional tangential stress (at point A)

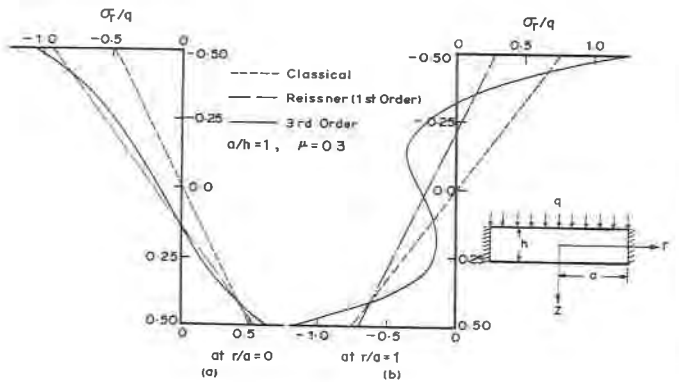

Fig. 4 Distribution of non-dimensional radial stress at r/a = 0 and r/a = 1.

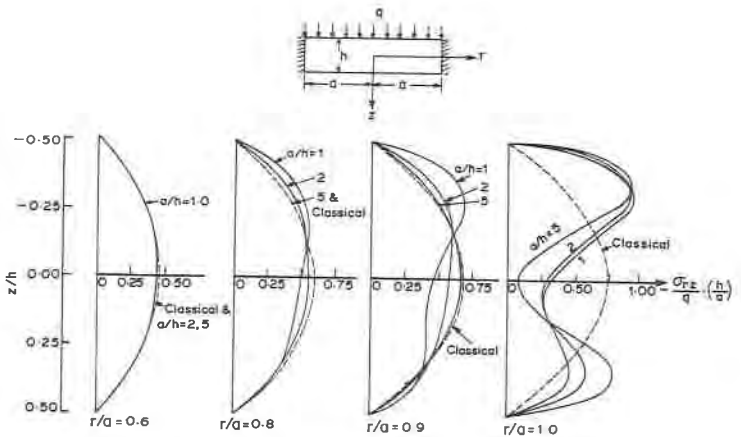

Fig. 5 Non-dimensional shear stress distribution at different sections for a/h = 1, 2 and 5.

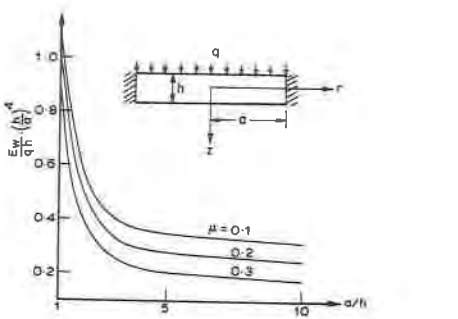

Fig. 6 Variation of maximum non-dimensional deflection for different Poisson's ratios.

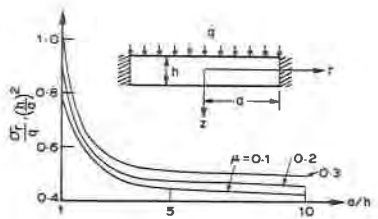

Fig. 7 Variation of non-dimensional radial stress at centre for z/h = - .5 for different Poisson's ratios.

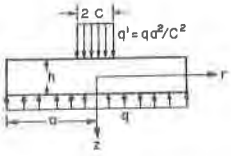

Fig. 8 Self-equilibrating normal loading on a solid circular plate

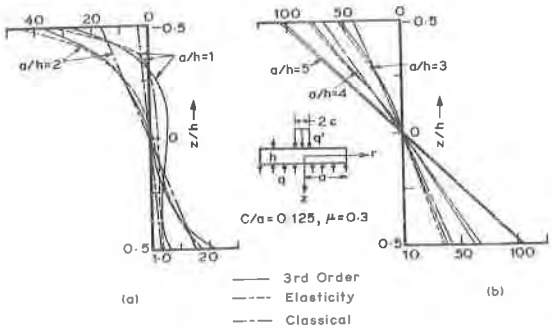

Fig. 9 Non-dimensional radial (or tangential) stress distribution along r/a = 0.

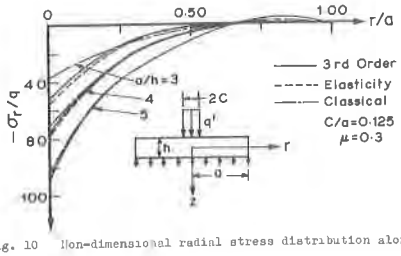

Fig. 10 Non-dimensional radial stress distribution along z/h =-.5

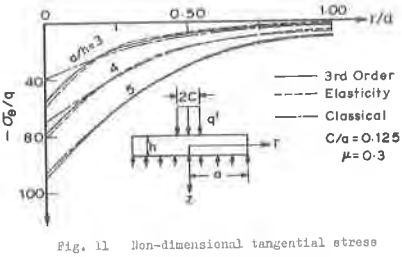

Fig. 11 Non-dimensional tangential stress distribution along z/h = - .5

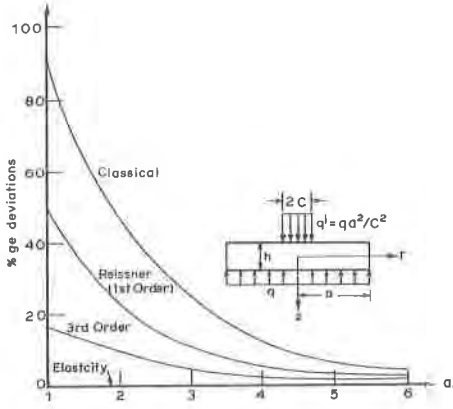

Fig. 12 Percentage deviations of radial stress at centre for z/h = .5 between various theories for different a/h ratios.